Supporting information

Manganese-rich High Entropy Oxides for Lithium-Ion Batteries:

Materials Design Approaches to Address Voltage Fade

Cynthia Huang[1,2]†, Jessica Luo[1,3]†, Zachary R. Mansley[4], Arun Kingan[1,2], Armando Rodriguez Campos[1,3], Zhongling Wang[1,2], Edelmy J. Marin Bernardez[1,3], Alexis Pace[1], Lu Ma[5], Steven N. Ehrlich[5], Lei Wang[1,4], David C. Bock[1,4], Esther S. Takeuchi[1,2,3,4], Amy C. Marschilok[1,2,3,4], Yimei Zhu[2,6], Shan Yan[1,4*], Kenneth J. Takeuchi[1,2,3,4*]

1. Institute of Energy: Sustainability, Environment, and Equity, Stony Brook University, Stony Brook, New York, 11794, United States.

2. Department of Materials Science and Chemical Engineering, Stony Brook University, Stony Brook, New York 11794, United States.

3. Department of Chemistry, Stony Brook University, Stony Brook, New York, 11794, United States.

4. Interdisciplinary Science Department, Brookhaven National Laboratory, Upton, NY 11973, United States.

5. National Synchrotron Light Source II, Brookhaven National Laboratory, Upton, NY 11973, United States.

6. Department of Condensed Matter Physics and Materials Science, Brookhaven National Laboratory, Upton, New York 11973, United States.

*corresponding authors (S.Y.) syan@bnl.gov, (K.J.T.) kenneth.takeuchi.1@stonybrook.edu

† CH and JL contributed equally to the manuscript

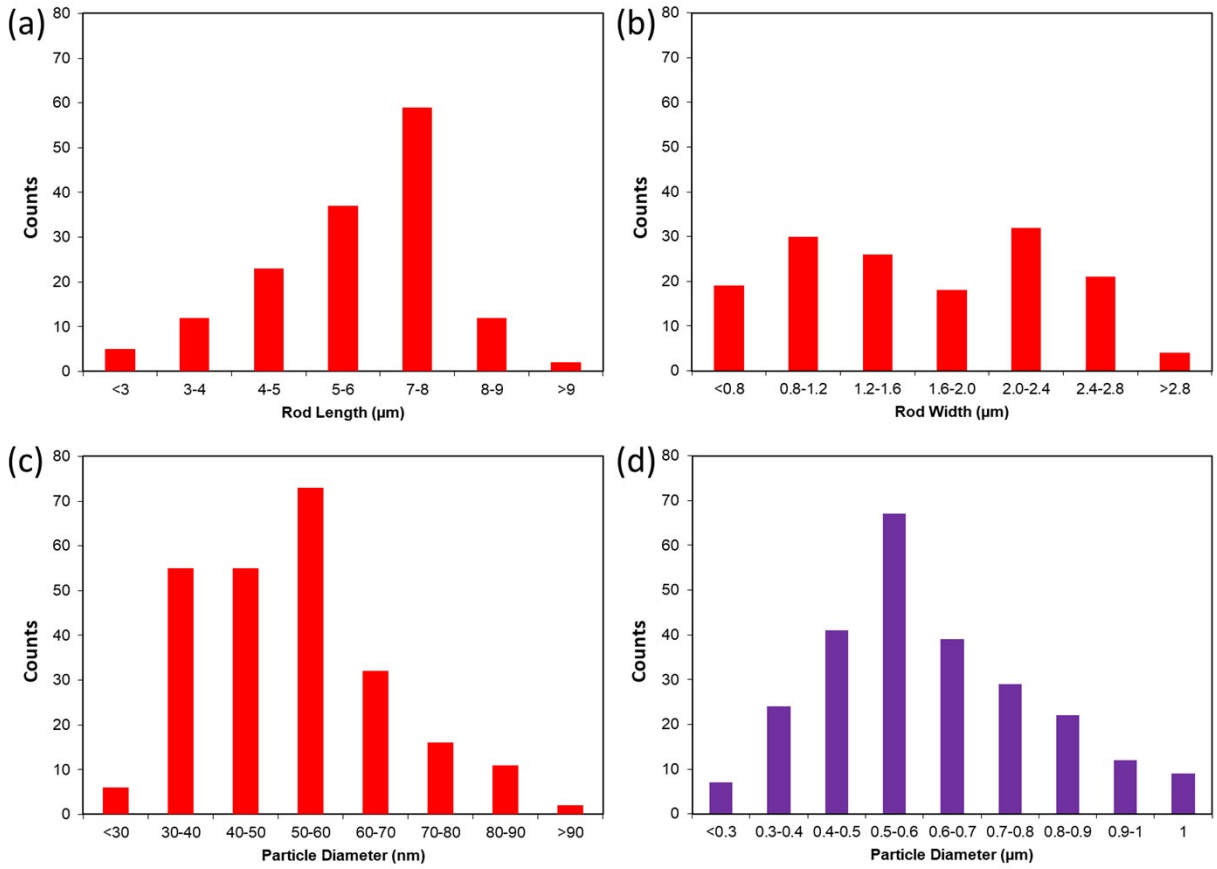

Figure S1. Size analysis of HEO-L (a-c) and HEO-H (d).

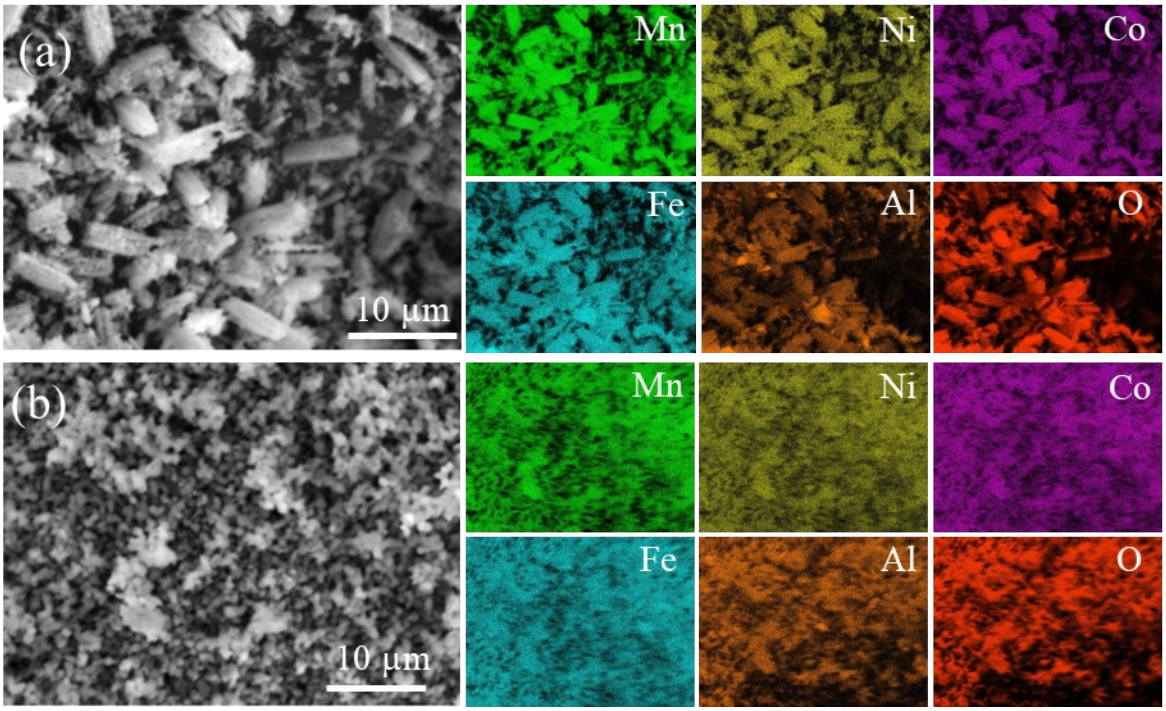

Figure S2. EDS images of HEO-L (a) and HEO-H(b).

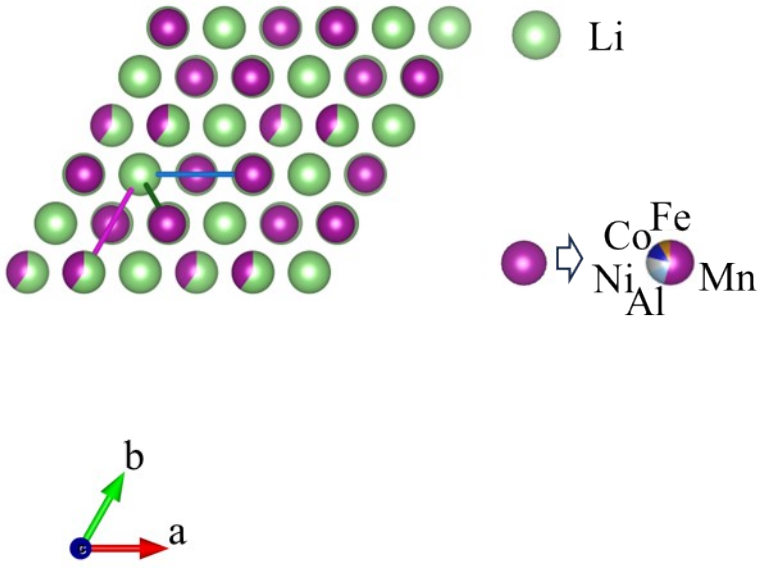

Figure S3. Schematic of HEO-L with stack faults with the stacking vectors viewed from the c axis.

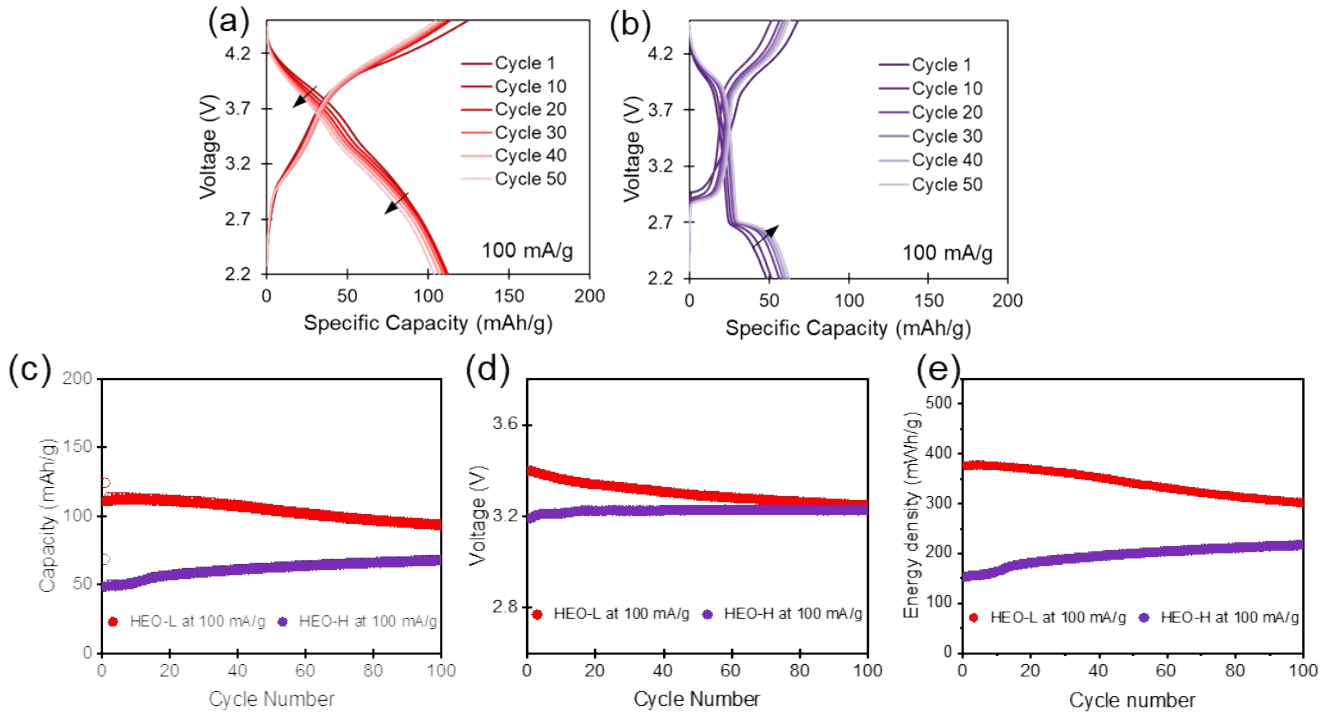

Figure S4. Electrochemistry of HEO-L and HEO-H cells at 100 mA/g after 3 formation cycles at 25 mA/g. (a-b) Voltage profiles of HEO-L (a) and HEO-H (b). (c) Extended cycle life of HEO-L and HEO-H, open circle indicates charge and solid cycle indicates discharge. (d) Average voltage of HEO-L and HEO-H. (e) Energy density at discharge of HEO-L and HEO-H.

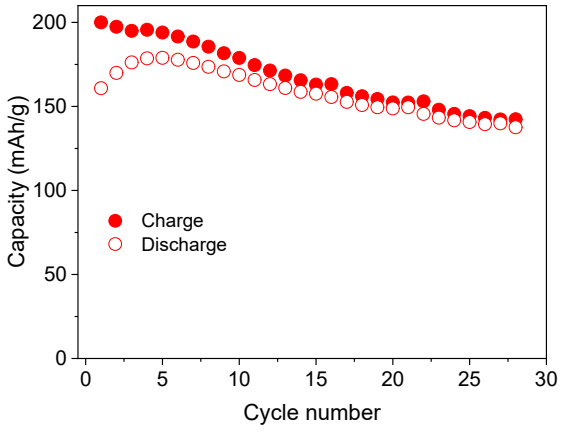

Figure S5. Galvanostatic cycling of lithium/ HEO-L cells at 10 mA/g.

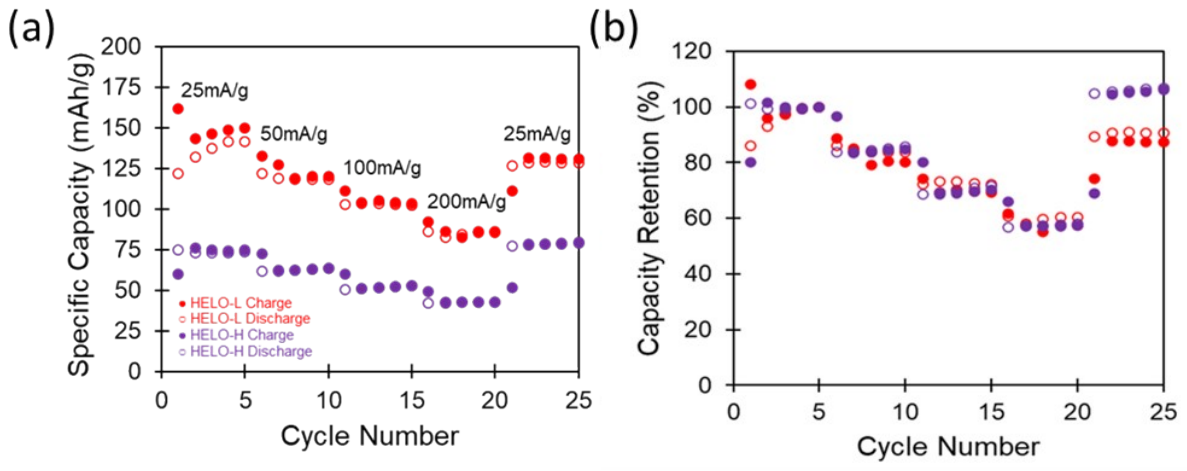

Figure S6. Rate capability of HEO-L (red) and HEO-H (purple) at 25, 50, 100, 200, and then back to 25mA/g, normalized by the 5th cycle, open circles indicate discharge and solid circles indicate charge.

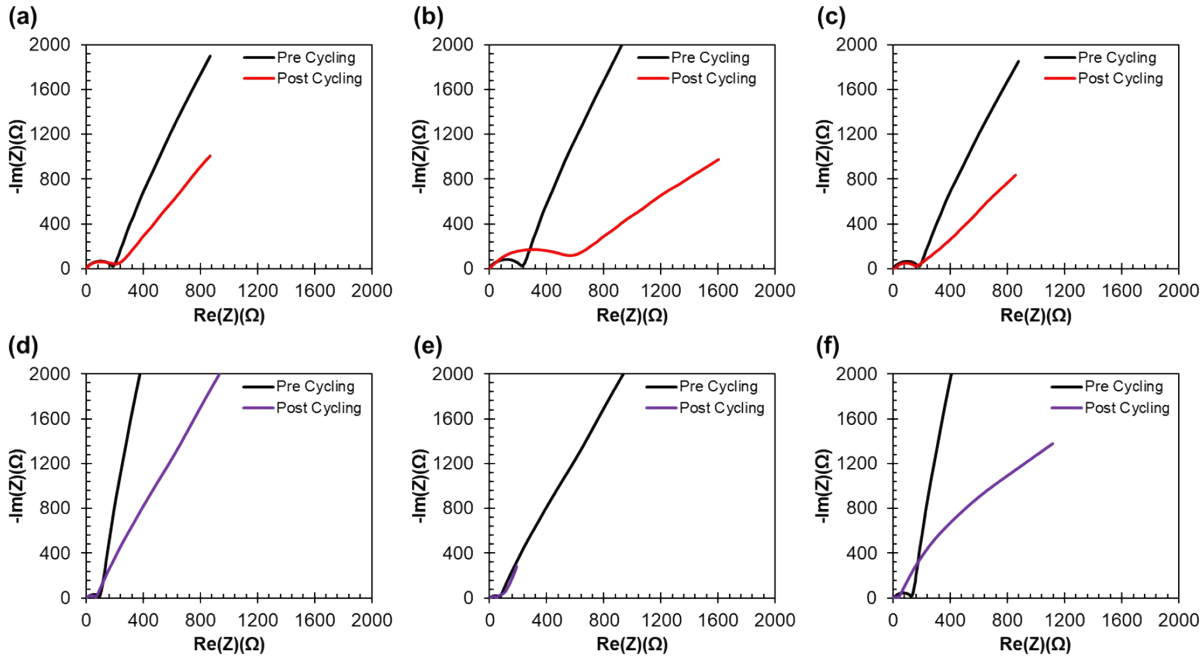

Figure S7. Electrochemical impedance spectroscopy recorded for cells before and after rate capability testing and galvanostatic cycling for 100 cycles. Top row: HEO-L before (black) and after (red) cycling under (a) rate capability testing, (b) 25 mA/g and (c) 100 mA/g. Bottom row: HEO-H before (black) and after (purple) cycling under (d) rate capability testing, (e) 25 mA/g and (f) 100 mA/g.

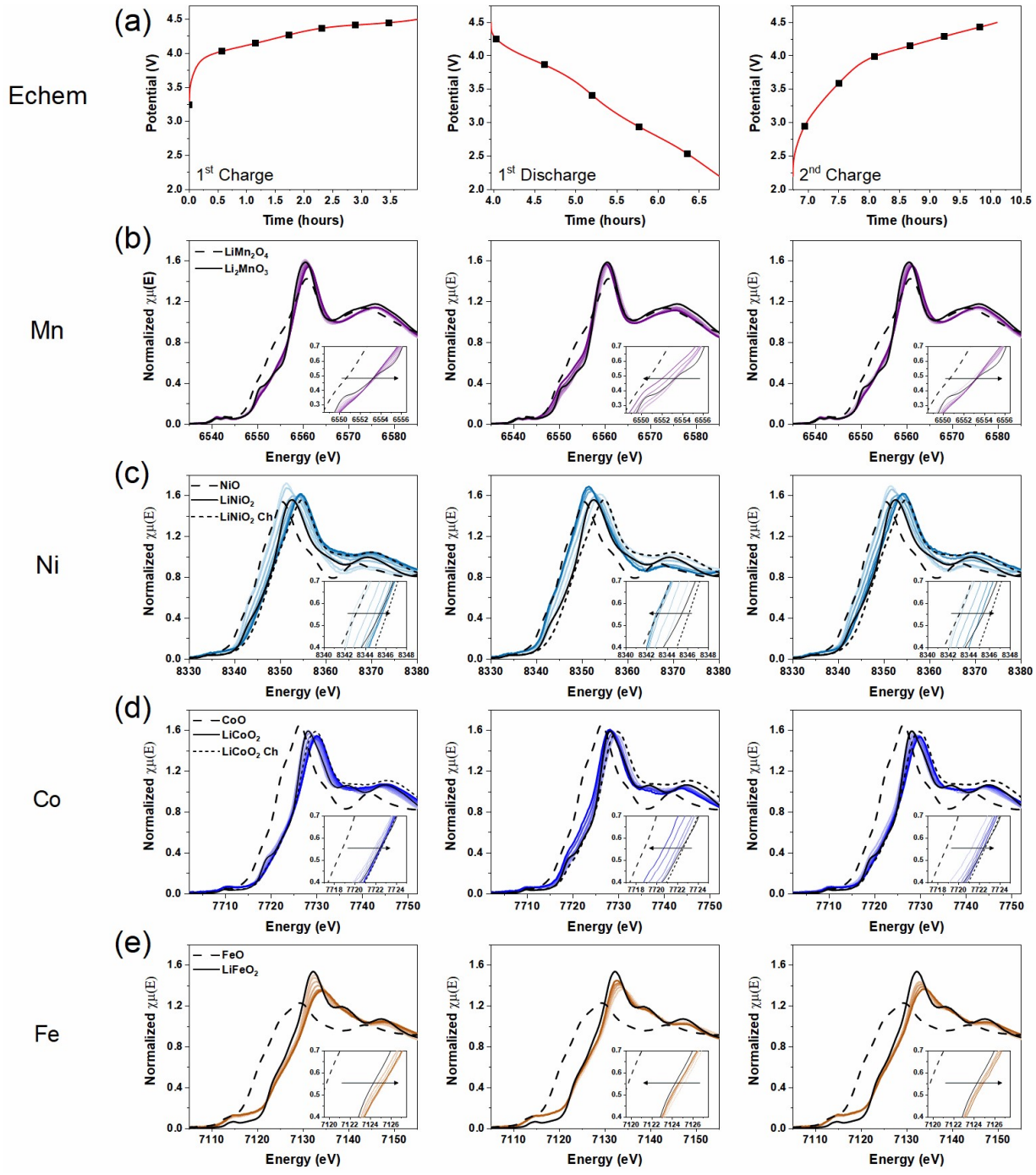

Figure S8. Operando XANES spectra of HEO-L electrodes in Li cells. (a) Galvanostatic cycling of HEO-L at current density of 30 mA/g. (b-e) *Operando* XANES spectra collected on Mn, Ni, Co and Fe K-edge of the cells.

Table S1. The composition of HEO-L-and HEO-H

HELO	ICP-OES	XANES/LCF				Composition
	Li : Mn : Ni : Co : Fe : Al	**Mn**	**Ni**	**Co**	**Fe**	
HEO-L	1.5 : 0.6 : 0.1 : 0.1 : 0.1 : 0.1	4.0	2.4	3.0	3.0	$Li_{1.5}Mn_{0.6}Ni_{0.1}Co_{0.1}Fe_{0.1}Al_{0.1}O_{2.5}$
HEO-H	0.5 : 0.6 : 0.1 : 0.1 : 0.1 : 0.1	3.8	2.4	2.7	3.0	$Li_{0.5}Mn_{0.6}Ni_{0.1}Co_{0.1}Fe_{0.1}Al_{0.1}O_{2.0}$

Table S2. Refined structural parameters of HEO-L.

R-Factor = 1.74 & χ2 = 22.91						
Unit cell parameters						
a,b (Å)		**c (Å)**			**γ (°)**	
4.92968 (1)		4.74505 (2)			60.12 (5)	
Atomic positions and occupancies						
Layer	**Atom**	**x/a**	**y/b**	**z/c**	**Occ.**	**B iso**
1	Li	0	0	0	1	1
	Li	1/3	1/3	0	1	1
	Li	2/3	2/3	0	1	1
2, 3, 4	Li	0	0	0	0.6	1
	Mn	0	0	0	0.4	1
	Mn	0.3292 (5)	0.3292 (5)	0	1	1
	Mn	0.6683 (1)	0.6683 (1)	0	1	1
	O	0.3368 (17)	-0.0051 (11)	0.2329 (5)	1	1
	O	0.6625 (1)	0.0002 (7)	-0.2300 (1)	1	1
	O	0.0050 (3)	0.3368 (1)	-0.2300 (1)	1	1
	O	0.3423 (11)	0.6554 (2)	-0.2249 (1)	1	1
	O	0.6552 (1)	0.3423 (1)	0.2281 (1)	1	1
	O	0.0034 (7)	0.6600 (1)	0.2326 (1)	1	1

Table S3. EXAFS fitting parameters for HEO-L sample measured at the Mn K-edge. E_0: shift in absorption edge energy. N: coordination number. R: interatomic distance. σ^2: Debye-Waller factor.

Theoretical FEFF	S_0^2	E_0 (eV)	Scattering Path	N	R (Å)	σ^2 (Å^2)	R-factor
Li_2MnO_3 (*C 2/m*)	0.67(9)	-3(2)	Mn-O	6	1.91(1)	0.002(2)	0.017
			Mn-Mn	2	2.89(1)	0.001(3)	
			Mn-Mn	1	3.14(5)	0.001(3)	
			Mn-Li	2	2.59(15)	0.001(3)	
			Mn-Li	4	2.99(1)	0.002(2)	
			Mn-Li	2	3.04(1)	0.002(2)	
			Mn-O	2	3.60(15)	0.02(3)	
			Mn-O	4	3.68(15)	0.02(3)	

Table S4. EXAFS fitting parameters for HEO-L sample measured at the Ni K-edge. E_0: shift in absorption edge energy. N: coordination number. R: interatomic distance. σ^2: Debye-Waller factor.

Theoretical FEFF	S_0^2	E_0 (eV)	Scattering Path	N	R (Å)	σ^2 (Å^2)	R-factor
Li_2MnO_3 (*C 2/m*)	0.85	-1(1)	Ni-O	6	2.03(1)	0.004(1)	0.014
			Ni-Mn	2	2.89(10)	0.001(1)	
			Ni-Mn	1	2.84(31)	0.001(1)	
			Ni-Li	2	2.61(24)	0.001(1)	
			Ni-Li	4	2.99(10)	0.001(1)	
			Ni-Li	2	3.04(10)	0.001(1)	
			Ni-O	2	3.26(4)	0.001(4)	
			Ni-O	4	3.35(4)	0.001(4)	

Table S5. EXAFS fitting parameters for HEO-L sample measured at the Co K-edge. E_0: shift in absorption edge energy. N: coordination number. R: interatomic distance. σ^2: Debye-Waller factor.

Theoretical FEFF	S_0^2	E_0 (eV)	Scattering Path	N	R (Å)	σ^2 (Å^2)	R-factor
Li_2MnO_3 (*C 2/m*)	0.72(10)	-4(2)	Co-O	6	1.92(1)	0.002(1)	0.019
			Co-Mn	2	2.84(22)	0.002(1)	
			Co-Mn	1	2.84(51)	0.002(1)	
			Co-Li	2	2.59(27)	0.002(1)	
			Co-Li	4	2.95(22)	0.002(1)	
			Co-Li	2	3.00(22)	0.002(1)	
			Co-O	2	3.34(23)	0.005(1)	
			Co-O	4	3.42(24)	0.005(1)	

Table S6. EXAFS fitting parameters for HEO-L sample measured at the Fe K-edge. E_0: shift in absorption edge energy. N: coordination number. R: interatomic distance. σ^2: Debye-Waller factor.

Theoretical FEFF	S_0^2	E_0 (eV)	Scattering Path	N	R (Å)	σ^2 (Å^2)	R-factor
Li_2MnO_3 (*C 2/m*)	0.90	-5(2)	Fe-O	6	1.98(2)	0.001(2)	0.020
			Fe-Mn	2	2.90(3)	0.002(2)	
			Fe-Mn	1	3.07(8)	0.001(2)	
			Fe-Li	2	2.81(8)	0.001(2)	
			Fe-Li	4	2.99(8)	0.001(2)	
			Fe-Li	2	3.04(8)	0.001(2)	

Table S7. Refined structural parameters of HEO-H.

Rwp = 2.79%					
Layered Phase					
Unit cell parameters	**a, b (Å)**	**c (Å)**	**Strain (%)**	**Weight Fraction (%)**	
	2.8867(4)	14.2294(11)	0.383 (19)	0.199 (2)	
Atomic positions and occupancies					
Atom	**x/a**	**y/b**	**z/c**	**Occ.**	**U iso**
Li	0	0	0.5	1.000	0.0100
O	0	0	0.2775(7)	1.000	0.0100
Mn	0	0	0	0.879(7)	0.0229(19)
Co	0	0	0	0.121(7)	0.0229(19)
Spinel Phase					
Unit cell parameters	**a, b, c (Å)**		**Strain (%)**	**Weight Fraction (%)**	
	8.1921(2)		0.720 (7)	0.801 (3)	
Atomic positions and occupancies					
Atom	**x/a**	**y/b**	**z/c**	**Occ.**	**U iso**
O	0.2584(2)	0.2584(2)	0.2584(2)	1.000	0.0140(15)
Li	0.125	0.125	0.125	0.783(4)	0.0227(32)
Co	0.125	0.125	0.125	0.217(4)	0.0227(32)
Ni	0.5	0.5	0.5	0.134	0.0110(6)
Mn	0.5	0.5	0.5	0.600	0.0110(6)
Al	0.5	0.5	0.5	0.135	0.0110(6)
Fe	0.5	0.5	0.5	0.131	0.0110(6)

Table S8. EXAFS fitting parameters for HEO-H sample measured at the Mn K-edge. S_0^2: amplitude reduction factor. E_0: shift in absorption edge energy. N: coordination number. R: interatomic distance. σ^2: Debye-Waller factor.

Theoretical FEFF	**S_0^2**	**Phase Fraction**	**E_0 (eV)**	**Scattering Path**	**N**	**R (Å)**	**σ^2 (Å^2)**	**R-factor**
Layered $R\bar{3}m$	0.61(6)	0.15	0(1)	Mn-O	6	1.93(1)	0.003(1)	0.019
				Mn-Mn	6	2.89(1)	0.005(1)	
				Mn-Li	6	2.90(1)	0.005(1)	
Spinel $Fd\bar{3}m$ Wyckoff site 16d	0.61(6)	0.85	0(1)	Mn-O	6	1.90(1)	0.001(3)	
				Mn-Mn	6	2.90(1)	0.002(2)	
				Mn-O	6	3.61(4)	0.02(3)	

Table S9. EXAFS fitting parameters for HEO-H sample measured at the Ni K-edge. E_0: shift in absorption edge energy. N: coordination number. R: interatomic distance. σ^2: Debye-Waller factor.

Theoretical FEFF	S_0^2	E_0 (eV)	Scattering Path	N	R (Å)	σ^2 (Å^2)	R-factor
Spinel (*Fd3m*), Wyckoff site 16d	0.80	-1(1)	Ni-O	6	2.03(1)	0.007(2)	0.011
			Ni-Mn	6	2.91(1)	0.007(2)	
			Ni-Mn	3	3.42(1)	0.007(2)	
			Ni-Li	3	3.42(1)	0.007(2)	
			Ni-O	6	3.47(7)	0.007(2)	

Table S10. EXAFS fitting parameters for HEO-H sample measured at the Co K-edge. E_0: shift in absorption edge energy. N: coordination number. R: interatomic distance. σ^2: Debye-Waller factor.

Theoretical FEFF	S_0^2	Phase Fraction	E_0 (eV)	Scattering Path	N	R (Å)	σ^2 (Å^2)	R-factor
Layered (*R-3m*)	0.61(6)	0.71(6)	1(1)	Co-O	6	1.93(1)	0.002(1)	0.021
				Co-Mn	6	2.87(1)	0.005(1)	
				Co-Li	6	2.87(1)	0.005(1)	
				Co-O	6	3.49(1)	0.005(1)	
				Co-O	6	4.201(2)	0.005(1)	
Spinel (*Fd3m*), Wyckoff site 8a	0.61(6)	0.29(6)	1(1)	Co-O	4	1.87(1)	0.002(1)	
				Co-Mn	12	3.38(1)	0.005(1)	
				Co-O	12	3.41(1)	0.005(1)	

Table S11. EXAFS fitting parameters for HEO-H sample measured at the Fe K-edge. E_0: shift in absorption edge energy. N: coordination number. R: interatomic distance. σ^2: Debye-Waller factor.

Theoretical FEFF	S_0^2	E_0 (eV)	Scattering Path	N	R (Å)	σ^2 (Å^2)	R-factor
Spinel (*Fd3m*), Wyckoff site 16d	0.81(12)	-7(1)	Fe-O	6	1.97(1)	0.007(2)	0.017
			Fe-Mn	6	2.94(1)	0.007(2)	
			Fe-Mn	3	3.54(3)	0.007(2)	
			Fe-Li	3	3.54(3)	0.007(2)	
			Fe-O	6	3.77	0.007(2)	

Table S12. Irreversible capacity values for cycles 1 and 2.

	HEO-L		HEO-H	
	Cycle 1 mAh/g	Cycle 2 mAh/g	Cycle 1 mAh/g	Cycle 2 mAh/g
Charge Capacity (mAh/g)	146.2	133.6	41.8	80.8
Discharge Capacity (mAh/g)	111.9	121.5	78.1	76.4
Irreversible capacity C minus D	34.3	12.1	-36.3	4.4
Irreversible capacity %	23%	9%	N/A	5.4%

Table S13. Comparisons of the delivered capacities under charge and discharge for related materials from the literature to this work.

Material, Synthesis	Structure	Current Density	1st Charge Capacity at < 4.45 V (mAh/g)	Voltage Range (V)	1st Cycle Charge Capacity (mAh/g)	1st Cycle Discharge Capacity (mAh/g)	Ref
HEO-L	**Layered**	**10 mA/g**	**177**	**2.2 – 4.5**	**200**	**161**	**This work**
$Li[Li_{0.2}Ni_{0.1}Co_{0.2}Mn_{0.5}]O_2$ Sol-gel, annealed at 950°C in air	Layered	0.4 mA/cm^2	~140	2.5 – 4.5	~260	190	[1]
$Li[Li_{0.2}Ni_{0.166}Co_{0.067}Mn_{0.567}]O_2$ Solid state, annealed between 500-1000°C in air	Layered	20 mA/g	108	2.0 – 4.6	302	224	[2]
$Li_{1.2}Ni_{0.16}Mn_{0.51}Al_{0.05}Co_{0.08}O_2$ Self-combustion, annealed between 450-900°C in air	Layered	25 mA/g	~120	2.0 – 4.6	320	215	[3]
$Li[Li_{0.1}Ni_{0.2}Co_{0.1}Mn_{0.6}]O_2$ Sol-gel, annealed at 950°C in air	Layered	0.1 mA/cm^2	~170	2.5 – 4.6	~275	~215	[4]
$Li_{1.2}Ni_{0.15}Mn_{0.55}Co_{0.1}O_2$ Commercial source	Layered	10 mA/g	~125	2.0 – 4.7	327	283	[5]
$Li[Li_{0.2}Ni_{0.2}Mn_{0.6}]O_2$ Coprecipitation, annealed at 900°C	Layered	10 mA/g	~110	2.0 – 4.7	330	281	[6]
HEO-H	**Layered -Spinel**	**25 mA/g**	**39**	**2.2 – 4.5**	**42**	**78**	**This work**
$Li_{1.2}Ni_{0.13}Co_{0.13}Mn_{0.54}O_2$-$LiNi_{0.5}Mn_{0.5}O_4$ Sol-gel, annealed at 750°C in air	Layered-Spinel	60 mA/g	~45-150	2.0 – 4.8	~250-325	~225-260	[7]
$Li_{1.1}[Mn_{0.6}Co_{0.8}Ni_{0.6}]O_{4-\sigma}$ Hydrothermal, annealed at 500-600°C	Layered-Spinel	~27 mA/g	~80-90	2.0 – 4.9	~240-349	~140-149	[8]
$Li_{1.17}Ni_{0.25}Mn_{1.08}O_3$ Self-combustion, annealed at	Layered-Spinel	20 mA/g	~35	2.4 – 4.9	130	140	[9]

900°C in air							
$0.75Li[Mn_{1.5}Ni_{0.5}]O_4 \cdot 0.25\{Li_2MnO_3 \cdot Li(Mn_{0.5}Ni_{0.5})O_2$ Coprecipitation, annealed at 900°C in air	Layered-Spinel	0.1 mA/cm^2	~40	2.0 – 4.95	~150	~200	[10]
$LiMn_{1.9}Al_{0.1}O_4$ Combustion, annealed at 850°C	Spinel	~70 mA/g	-	3.2 – 4.2	100.7	89.5	[11]
$LiMn_2O_4$ doped with Cu/Al/Ti Sol-gel, annealed at 800°C	Spinel	~15 mA/g	-	3.5 – 4.3	-	134	[12]
$LiMn_2O_4$ Solid state, annealed at 800°C	Spinel	~20 mA/g	~125	3.4 – 4.5	~130	125	[13]
$LiNi_{0.5}Mn_{1.5}O_4$ Solid state, annealed between 500-900°C in air	Spinel	~15 mA/g	~25	3.5 – 4.9	140	120	[14]

References

1. K. S. Park, M. H. Cho, S. J. Jin and K. S. Nahm, *Electrochem Solid St*, 2004, **7**, A239-A241.
2. H. J. Yu, H. J. Kim, Y. R. Wang, P. He, D. Asakura, Y. Nakamura and H. S. Zhou, *Phys Chem Chem Phys*, 2012, **14**, 6584-6595.
3. P. K. Nayak, J. Grinblat, M. Levi, E. Levi, S. Kim, J. W. Choi and D. Aurbach, *Advanced Energy Materials*, 2016, **6**.
4. J. H. Kim, C. W. Park and Y. K. Sun, *Solid State Ionics*, 2003, **164**, 43-49.
5. M. Bettge, Y. Li, K. Gallagher, Y. Zhu, Q. Wu, W. Lu, I. Bloom and D. P. Abraham, *Journal of The Electrochemical Society*, 2013, **160**, A2046-A2055.
6. J. M. Zheng, W. Shi, M. Gu, J. Xiao, P. J. Zuo, C. M. Wang and J. G. Zhang, *Journal of the Electrochemical Society*, 2013, **160**, A2212-A2219.
7. X. Feng, Z. Z. Yang, D. C. Tang, Q. Y. Kong, L. Gu, Z. X. Wang and L. Q. Chen, *Phys Chem Chem Phys*, 2015, **17**, 1257-1264.
8. L. H. Hu, L. Yin, F. Hassan and J. Cabana, *J Solid State Chem*, 2020, **288**.
9. P. K. Nayak, J. Grinblat, M. Levi, O. Haik, E. Levi, Y. K. Sun, N. Munichandraiah and D. Aurbach, *Journal of Materials Chemistry A*, 2015, **3**, 14598-14608.
10. S. H. Park, S. H. Kang, C. S. Johnson, K. Amine and M. M. Thackeray, *Electrochem Commun*, 2007, **9**, 262-268.
11. Z. F. Cai, Y. Z. Ma, X. N. Huang, X. H. Yan, Z. X. Yu, S. H. Zhang, G. S. Song, Y. L. Xu, C. E. Wen and W. D. Yang, *J Energy Storage*, 2020, **27**.
12. L. L. Xiong, Y. L. Xu, T. Tao and J. B. Goodenough, *J Power Sources*, 2012, **199**, 214-219.
13. J. Cho and M. M. Thackeray, *Journal of the Electrochemical Society*, 1999, **146**, 3577-3581.

14. J. H. Kim, N. P. W. Pieczonka, Z. C. Li, Y. Wu, S. Harris and B. R. Powell, *Electrochim Acta*, 2013, **90**, 556-562.